The Astrophysical Journal Letters, 711:L12–L18, 2010 March 1 doi:10.1088/2041-8205/711/1/L12

ON THE FLARE INDUCED HIGH-FREQUENCY GLOBAL WAVES IN THE SUN

Brajesh Kumar[1], Savita Mathur[2], R. A. García[3], and P. Venkatakrishnan[1]
[1] Udaipur Solar Observatory, Physical Research Laboratory, Dewali, Badi Road, Udaipur 313 004, India; brajesh@prl.res.in, pvk@prl.res.in
[2] Indian Institute of Astrophysics, Koramagala, Bangalore 560 034, India; smathur@iiap.res.in
[3] Laboratoire AIM, CEA/DSM-CNRS, Université Paris 7 Diderot, IRFU/SAp, Centre de Saclay, 91191, Gif-sur-Yvette, France; rafael.garcia@cea.fr
Received 2009 November 27; accepted 2010 January 21; published 2010 February 10

ABSTRACT

Recently, Karoff & Kjeldsen presented evidence of strong correlation between the energy in the high-frequency part ($5.3 < \nu < 8.3$ mHz) of the acoustic spectrum of the Sun and the solar X-ray flux. They have used disk-integrated intensity observations of the Sun obtained from the Variability of solar IRradiance and Gravity Oscillations instrument on board *Solar and Heliospheric Observatory* (*SOHO*) spacecraft. Similar signature of flares in velocity observations has not been confirmed till now. The study of low-degree high-frequency waves in the Sun is important for our understanding of the dynamics of the deeper solar layers. In this Letter, we present the analysis of the velocity observations of the Sun obtained from the Michelson and Doppler Imager (MDI) and the Global Oscillations at Low Frequencies (GOLF) instruments on board *SOHO* for some major flare events of the solar cycle 23. Application of wavelet techniques to the time series of disk-integrated velocity signals from the solar surface using the full-disk Dopplergrams obtained from the MDI clearly indicates that there is enhancement of high-frequency global waves in the Sun during the flares. This signature of flares is also visible in the Fourier Power Spectrum of these velocity oscillations. On the other hand, the analysis of disk-integrated velocity observations obtained from the GOLF shows only marginal evidence of effects of flares on high-frequency oscillations.

Key words: Sun: atmosphere – Sun: flares – Sun: oscillations

Online-only material: color figures

1. INTRODUCTION

In the Sun, the typical distribution of acoustic power of photospheric oscillations peaks at around 5 minutes (Leighton et al. 1962) with a general decrease to negligible power at higher frequencies. This behavior of the acoustic spectrum has been understood in terms of trapped oscillations in a cavity (Ulrich 1970; Leibacher & Stein 1971). The eigenfunctions corresponding to the band of oscillations in the region of 5 minutes peak in the convection zone, which seems to be the dominant source of excitation of the solar oscillations (Goldreich et al. 1994). Apart from these normal modes of oscillations (*p*-modes), researchers have found the presence of high-frequency oscillations (frequencies higher than the solar-photospheric acoustic cutoff at about 5.3 mHz) in the solar-acoustic spectrum (Libbrecht & Kaufman 1988; Libbrecht 1988; Chaplin et al. 2003; Jiménez et al. 2005; Karoff & Kjeldsen 2008). Unlike the normal *p*-modes, the driving mechanism of these high-frequency solar oscillations is still not well established. Balmforth & Gough (1990) suggest that the high-frequency waves are partly reflected by a sudden change in temperature at the transition region between the chromosphere and the corona. Kumar & Lu (1991) explain these high-frequency waves as an interference phenomenon between ingoing and outgoing waves from a localized source just beneath the photosphere.

Wolff (1972) suggested that large solar flares can stimulate free modes of oscillation of the entire Sun, by causing a thermal expansion that would drive a compression front to move into the solar interior. Several researchers have tried to study the effect of flares on the acoustic-velocity oscillations of the Sun. The progress in this field escalated recently with the advent of continuous data from dedicated instruments such as Michelson and Doppler Imager (MDI; Scherrer et al. 1995) on board *Solar and Heliospheric Observatory* (*SOHO*) spacecraft and Global Oscillation Network Group (GONG; Harvey et al. 1995). Haber et al. (1988) reported an average increase in the power of intermediate-degree modes after a major flare (of class X13/3B) using a few hours of solar-oscillations data obtained by the Dunn telescope at National Solar Observatory/ Sacramento Peak, USA. Braun & Duvall (1990) could not detect acoustic-wave excitation from an X-class flare. Kosovichev & Zharkova (1998) reported the first detection of "solar quakes" inside the Sun, caused by the X2.6 flare of 1996 July 9, using the MDI Dopplergrams. Following this result, Donea et al. (1999) found an acoustic source associated with a flare using seismic images produced with the helioseismic-holography technique. Application of ring-diagram analysis showed that the power of the global *p*-modes appears to be larger in several flare-producing active regions as compared with the power in non-flaring regions of similar magnetic field strength (Ambastha et al. 2003).

Additionally, Donea & Lindsey (2005) have reported emission of seismic waves from large solar flares using helioseismic holography. Some of the large solar flares have been observed to produce enhanced high-frequency acoustic velocity oscillations in localized parts of active regions (Kumar & Ravindra 2006). Further, Zharkova & Zharkov (2007) reported large downflows associated with seismic sources during the major flare (of class X17.6/4B) of 2003 October 28. Venkatakrishnan et al. (2008) report cospatial evolution of seismic sources and Hα flare kernels during the aforementioned flare event. A search for a correlation between the energy of the low-degree *p*-modes and flares using velocity observations of the Sun remained inconclusive (Gavryusev & Gavryuseva 1999; Chaplin et al. 2004; Ambastha & Antia 2006). The study of low-degree high-frequency (LDHF) waves in the Sun is important as this can bring more constraints on the rotation profile between 0.1 and 0.2 R_O (García et al. 2008; Mathur et al. 2008). The effect of flares on such LDHF waves can provide a clue to the origin of these waves.

Recently, Karoff & Kjeldsen (2008) have reported that the correlation between X-ray flare intensity and the energy in the acoustic spectrum of disk-integrated intensity oscillations (as observed with Variability of Solar IRradiance and Gravity (VIRGO; Fröhlich et al. 1995) instrument on board *SOHO*) is stronger for high-frequency waves than that for the well-known 5-minute oscillations. This correlation was obtained for a long time series of eight years with time variation of power smoothed with a 24-day filter. This result does not show the immediate consequence of individual flares. For this, we require shorter time series closely associated with the flares. Since, the power spectra are noisier for shorter time series, we need to apply wavelet analysis to the time series. Intensity variations are generally manifestations of pressure variations. However, for a medium stratified by gravity, the waves are not pure acoustic waves, but are acousto-gravity waves. Hence, it will be more profitable to look at the velocity oscillations of the solar atmosphere. Therefore, in this study, we have searched for the effects of flares in the time series of disk-integrated velocity signals from the solar surface using the full-disk Dopplergrams obtained from the MDI instrument. We have also looked for these effects in disk-integrated velocity observations obtained from the Global Oscillation at Low Frequency (GOLF; Gabriel et al. 1995, 1997) instrument on board *SOHO*. These studies have been applied to the major solar flares of 2003 October 28 (of class X17.6/4B), 2003 October 29 (of class X10/2B), and 2001 April 6 (of class X5.6/3B) that occurred in the solar cycle 23. Each of the selected events is in decreasing order of flare strength as observed in X-ray (1–8 Å) by *GOES* (Geostationary Operational Environmental Satellite) (García 1994) satellites. Wavelet and Fourier analyses of MDI velocity observations clearly indicate the enhancement in high-frequency global waves in the Sun during the flares. However, this signature of flares is weaker in the case of GOLF as compared to MDI data.

2. DATA AND ANALYSIS

2.1. MDI Data

We have used the sequence of MDI full-disk Dopplergrams for three hours spanning the flare obtained on 2003 October 28 (10:00–13:00 UT), 2003 October 29 (19:00–22:00 UT), and 2001 April 6 (18:00–21:00 UT) with a cadence of 1 minute and a spatial sampling rate of 2 arcsec per pixel. We have also used three hours of MDI Dopplergrams for a quiet period (non-flaring condition) as control data. In order to compare the temporal behavior with the disk-integrated intensity observations by VIRGO, we have summed up the velocity signals over all the pixels of the MDI full-disk Dopplergrams. The images are first examined for pixels having cosmic-ray hits and such pixels are replaced by interpolation. A two-point backward difference filter (difference between two consecutive measurements) is applied to these sequences of images to enhance the velocity signals from the *p*-modes and high-frequency waves above the solar background. The sequence of these filtered Doppler images is then collapsed into a single velocity value, excluding the noisy pixels along the solar limb. This process is applied to the time series of Doppler images for all the three aforementioned flare events as well as the quiet period. It is believed that by collapsing the full-disk Doppler images, the acoustic modes with maximum $l = 0, 1, 2, 3$ remain while the modes higher than these are averaged out. Thus, the collapsed velocity value should be the representative of the global acoustic modes. The temporal evolution of these disk-integrated velocity signals for three hours spanning the flare is shown in the upper panel of Figures 1(a), 2(a), and 3(a) and that for the quiet period is shown in Figure 4(a).

2.2. GOLF Data

GOLF instrument measures the disk-integrated line-of-sight velocity of the Sun at a cadence of one raw count every 10 s. However, we have rebinned the velocity data from GOLF for every 60 s to match with MDI. We have used the same periods of data from both instruments for the flare events of 2003 October 28, 2003 October 29, and 2001 April 6, and for the non-flaring condition. We have worked with the standard velocity time series (García et al. 2005; Ulrich et al. 2000) as well as the original raw-counting rates. We have also checked if there was any anomalous behavior during the analyzed periods of time in the housekeeping data. Indeed, during the flare events of 2003 October 28–29, GOLF raw-counting rates of both photomultipliers suffered an increase in the measurements probably as a consequence of the impact of high-energetic particles. Due to these contaminations, the standard velocity time series have been filtered out during this period and thus, we have been obliged to work with the raw observations obtained by GOLF during the aforementioned flare events. A two-point backward difference filter is applied to the velocity series to remove the effect of the rotation and other slowly varying solar features. The temporal evolution of these filtered velocity signals for three hours spanning the flare is shown in the upper panels of Figures 1(b), 2(b), and 3(b) and that for the quiet period is shown in Figure 4(b).

2.3. Wavelet Analysis of MDI and GOLF Velocity Data

For the time–frequency analysis of the influence of flares on the high-frequency acoustic modes, we have applied the Wavelet technique (Torrence & Compo 1998) on the velocity time series obtained from MDI and GOLF as described above. We have used the Morlet wavelet, which is the product of a sine wave and a Gaussian function. We have computed the Wavelet Power Spectrum (WPS), which yields the correlation between the wavelet with a given frequency and the data along time. For the different events and the two instruments, we note the presence of power around 3 mHz, corresponding to the region of the normal *p*-modes. Concerning the high-frequency waves above 5 mHz, we can study the evolution of their power with time. We limit our study to the region inside a "cone of influence" corresponding to the periods of less than 25% of the time series length for reliability of the periods. Finally, we have also calculated two confidence levels of detection corresponding to the probability of 90% and 50% that the power is not due to noise. Thus, we have outlined the regions in the WPS where power lies above these confidence levels and these regions are shown in middle panels of Figures 1–4(a) and (b). A comparison of the WPS for the flare events with that of the quiet period clearly indicates the enhancement of high-frequency waves during these flare events as seen in the data from MDI instrument. However, in the case of GOLF data, some short-lived high-frequency waves are sporadically observed during the flares.

The WPS is collapsed along time to obtain the Global-wavelet power spectrum (GWPS). If some power is present during the whole length of our time series, it would easily be seen in the GWPS. This is nearly similar to the commonly used power spectral density. In Figures 1–4(a) and (b), the GWPS shows a

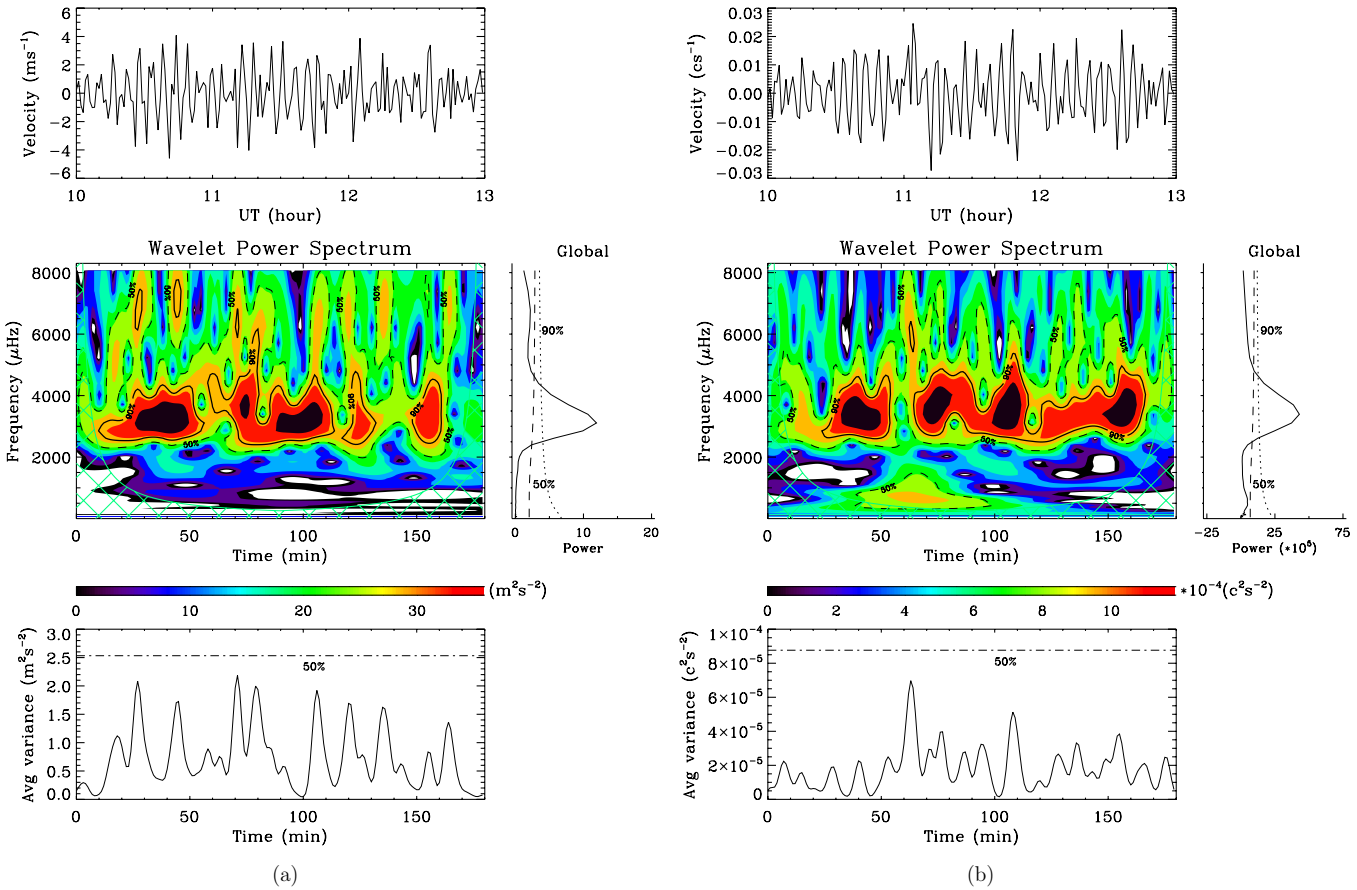

Figure 1. (a) Upper panel shows the temporal evolution of disk-integrated velocity signals obtained from the full-disk Dopplergrams observed by MDI during 10:00–13:00 UT spanning the flare event of 2003 October 28. Middle panels show the Wavelet Power Spectrum (WPS) and the Global-Wavelet Power Spectrum (GWPS) computed from this time series. In the WPS, the solid lines correspond to regions with the 90% confidence level whereas the dashed lines are for the 50% confidence level, and the hatched region indicates the cone of influence. The color scale is for the wavelet power. In the GWPS, the dotted line is for the 90% significance level and the dashed line is for the 50% significance level. Bottom panel illustrates the scale-average time series for the WPS in the frequency regime 5–8 mHz. The dashed-dotted line corresponds to the 50% significance level of the average variance. (b) Same as above, but using GOLF data.

(A color version of this figure is available in the online journal.)

strong peak of the normal *p*-modes which are well known to be existing all the time. However, if the power of high-frequency waves increases only a few times along the three hours of the studied data, this would not appear as a strong peak in the GWPS. In the case of MDI data, the GWPS for all the three flare events do show a bump corresponding to the high-frequency waves (above 5 mHz). Here again, we have overplotted the significance levels corresponding to probabilities of 90% and 50%. We note that the normal *p*-mode peak in the GWPS is above the 90% significance level whereas the high-frequency peak is just below the 50% significance level, i.e., it has at least 50% probability of being due to noise. However, the GWPS estimated from the MDI velocity data during a quiet period (Figure 4(a)) does not show any peak beyond 5 mHz. This supports the idea that the increase of power in the high-frequency regime of the GWPS is indeed caused by the flare. In the case of GOLF data, we do not observe this signature in the GWPS estimated for the flare events as the overall high-frequency signal is weak in these observations.

To see when the high-frequency waves have an increased power during the flare, we have calculated the scale-average time series in the frequency regime 5–8 mHz. Basically, it is a collapsogram of the WPS along the frequency of the wavelet in the chosen range. For this quantity, we have calculated the confidence level for a 50% probability. These are shown in the lower panels of Figures 1–4(a) and (b). Here, we observe peaks corresponding to the presence of high-frequency waves in the WPS. In general, the MDI data show more closely spaced high-amplitude peaks as compared to the GOLF data for the flare events, but still mainly around the 50% confidence level. A comparison with the same analysis performed for a quiet period (non-flaring condition) neither shows a high-frequency bump beyond 5 mHz in the GWPS (for MDI data) nor high-amplitude peaks in the scale-average time series (for both, MDI and GOLF data). Thus, in spite of the small confidence levels found during this analysis, it indicates a possible relationship between these excess high-frequency power and the flares.

2.4. Fourier Analysis of MDI and GOLF Velocity Data

We have also estimated the Fourier Power Spectrum (FPS) from the velocity time series obtained by the MDI and GOLF instruments for the aforementioned flare events and the quiet period. The FPS spectra obtained from the MDI and GOLF data are respectively shown in the left and right panels of Figure 5. In the estimation of FPS spectra, the Power Spectral Density has not been corrected for the transfer function of the two-point backward difference filter (García & Ballot 2008). A correction from the backward difference filter will change the slope, thereby affecting the relative amplitudes between

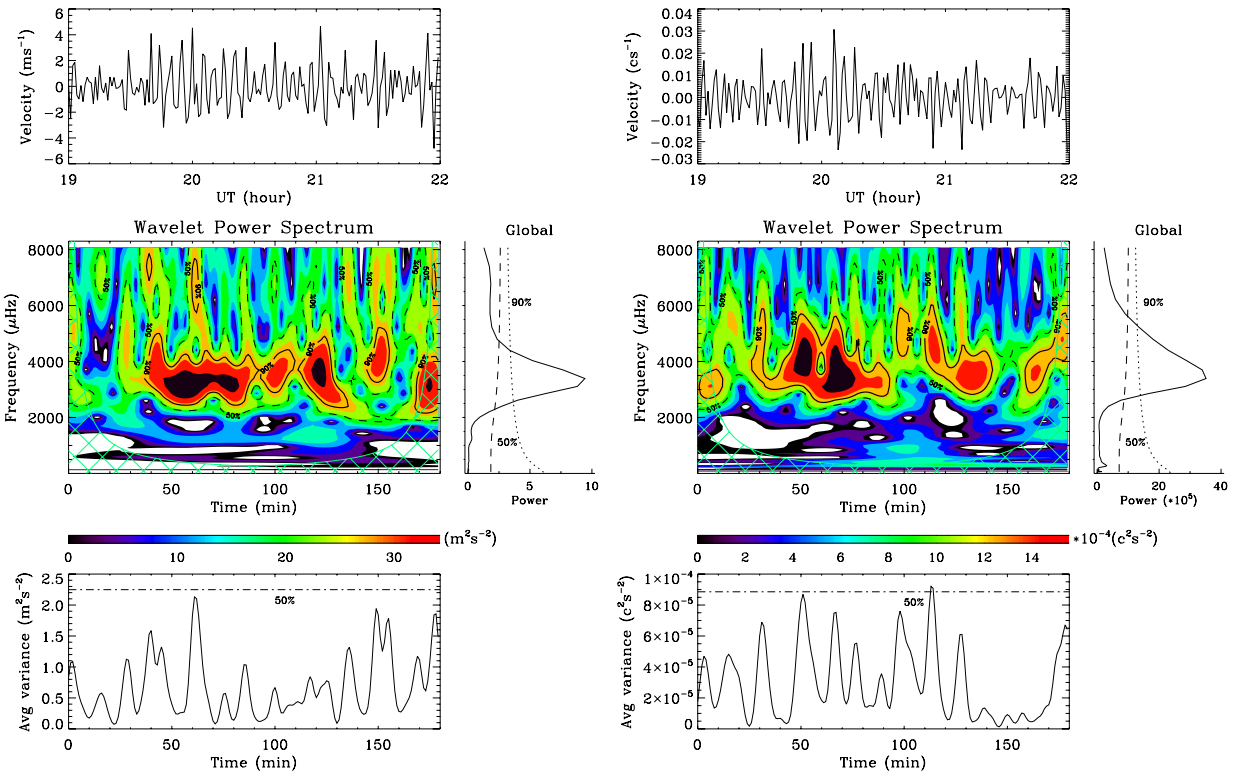

Figure 2. Same as Figure 1, but for the flare event of 2003 October 29 during 19:00–22:00 UT using (a) MDI data and (b) GOLF data.
(A color version of this figure is available in the online journal.)

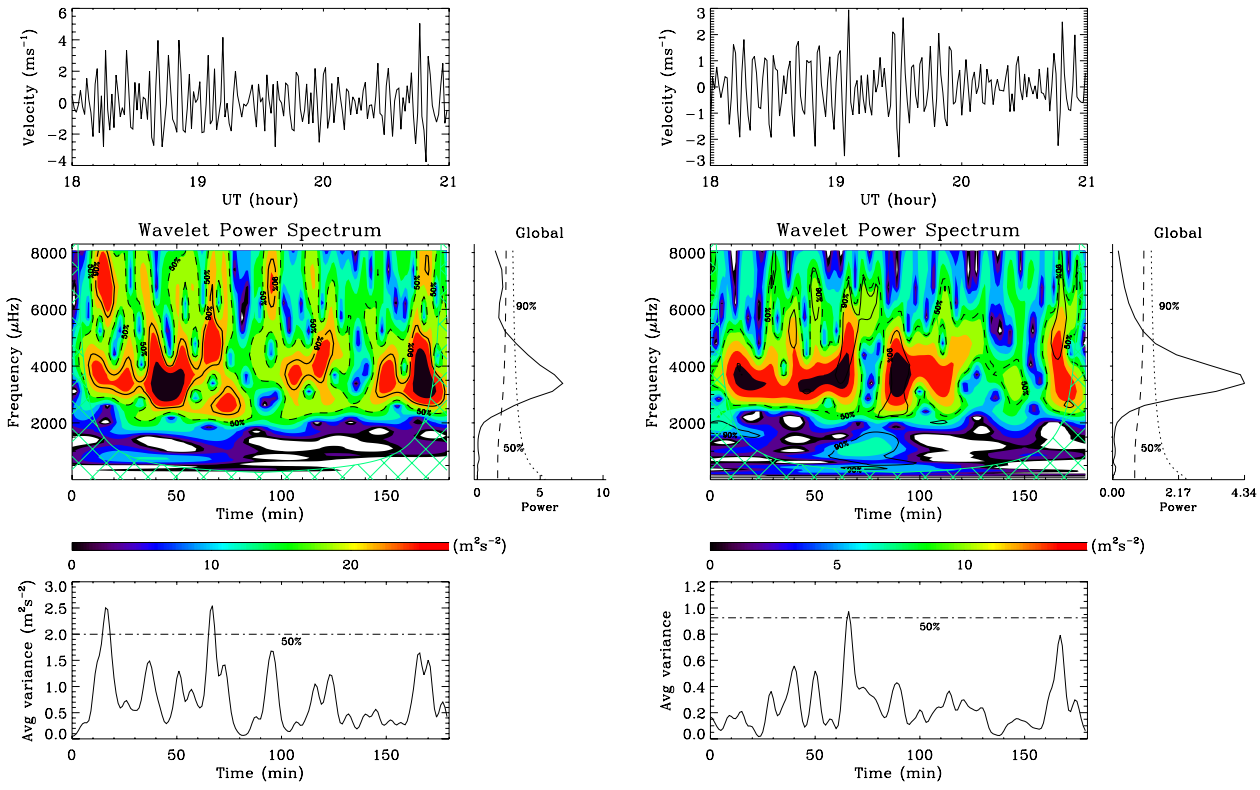

Figure 3. Same as Figure 1, but for the flare event of 2001 April 6 during 18:00–21:00 UT using (a) MDI data and (b) GOLF data.
(A color version of this figure is available in the online journal.)

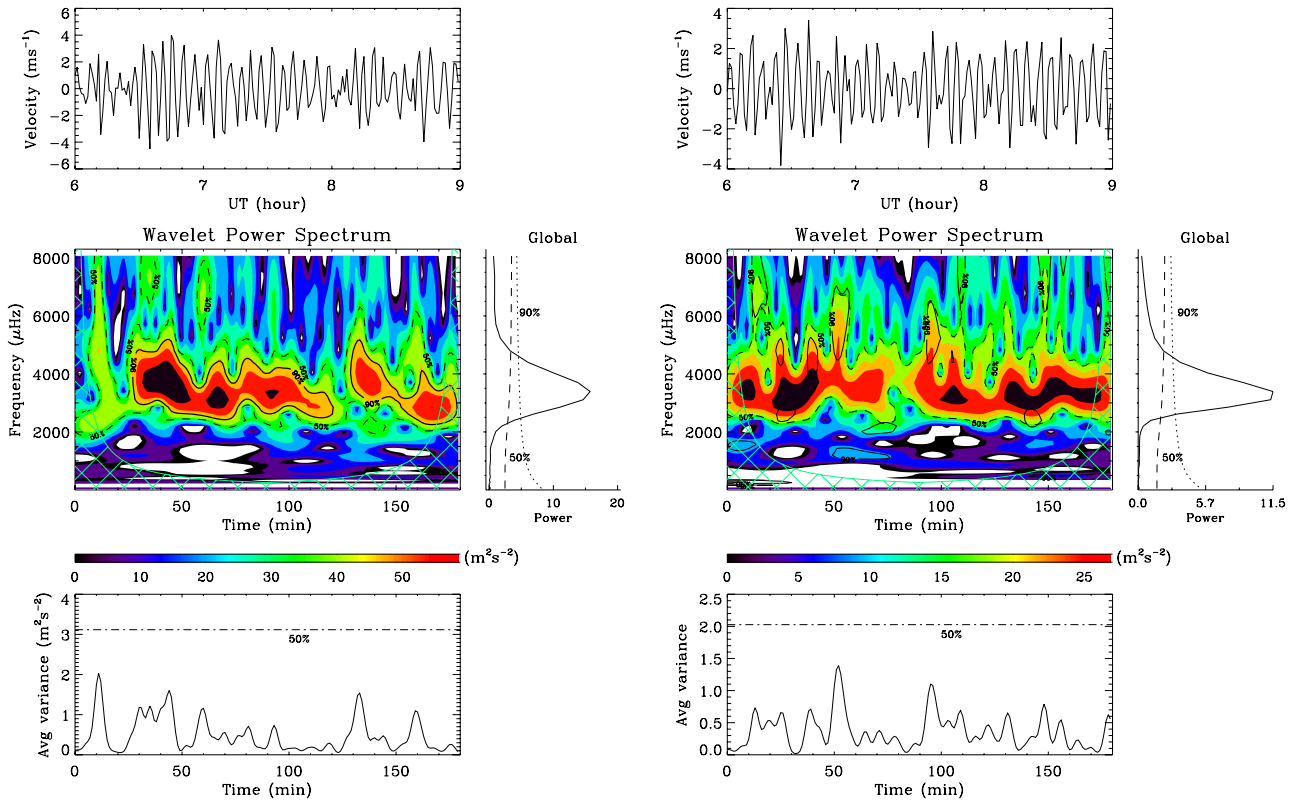

Figure 4. Same as Figure 1, but for a quiet period (non-flaring condition) using (a) MDI data and (b) GOLF data.
(A color version of this figure is available in the online journal.)

the normal *p*-modes and the high-frequency waves. Here, we study the high-frequency waves in an absolute manner for each event and we do not compare them with the normal *p*-modes. Therefore, it does not bias our study. The FPS shown in Figure 5 depicts dominant power in the 3 mHz band which is due to the normal *p*-modes. These FPS also show significant peaks in the higher frequency band (above 5 mHz) as estimated from MDI data for all the three flare events (strongest for the 2001 April 6 flare event). However, the GOLF data show the strong signature only for the flare event of 2003 October 29. The enhancement of high-frequency power related to the flare of 2003 October 28 has already been seen in the GONG velocity data (Kumar & Venkatakrishnan 2009). Here, we do observe spikes at high frequency in the FPS from the MDI data and some smaller ones from the GOLF data for these flare events. These spikes are very weak in the case of a quiet period, as seen in both the data sets (cf. bottom panels of Figure 5).

The difference found between the measurements of the two instruments could be a direct consequence of the different heights of the solar atmosphere sampled by each instrument (Ni I v/s Sodium doublet). The GOLF is observing in the high photosphere and the low chromosphere while the MDI or the GONG observes mostly in the deep photosphere close to where VIRGO is observing. Further analysis will be necessary to understand all the particularities of each seismic measurements (cf. Jiménez-Reyes et al. 2007).

3. DISCUSSION AND CONCLUSIONS

The existence of high-frequency acoustic waves was first discovered in high-degree observations at the Big Bear Solar Observatory (Libbrecht & Kaufman 1988; Libbrecht 1988) and later in GOLF low-degree disk-integrated observations (García et al. 1998). Recently, they have also been seen in BiSON disk-integrated radial-velocity data (Chaplin et al. 2003) and VIRGO intensity data (Jiménez et al. 2005). However, earlier attempts to find a correlation between the energy of these high-frequency oscillations and flares using disk-integrated velocity observations of the Sun had remained unclear (Gavryusev & Gavryuseva 1999; Chaplin et al. 2004). In our analysis, the enhancement of high-frequency power is clearly seen in the MDI velocity data (and a feeble enhancement is also seen in the GOLF velocity data) during the major flare events. It is comparable with the flare-related enhancements reported by Karoff & Kjeldsen (2008) in disk-integrated intensity oscillations as observed with VIRGO. Although, in our results the flare-induced enhancement signals are seen with a low probability (around 50%), this signature is larger than that seen in non-flaring condition for both the MDI and GOLF data.

Basically, two models have been proposed to account for these LDHF oscillations with frequencies higher than the photospheric acoustic cutoff frequency (∼5.3 mHz). The first model proposed by Balmforth & Gough (1990) suggests that the high-frequency waves are partially reflected at the transition region in comparison to the photospheric reflection for ordinary *p*-modes. The other model proposed by Kumar & Lu (1991) explains the high-frequency waves as an interference phenomenon between ingoing and outgoing waves from a localized source just beneath the photosphere. In either case, the amount of energy that is stored in the high-frequency waves is extremely low compared to the amount of energy stored in the normal *p*-modes which are powered by the strong turbulence in the convection zone of

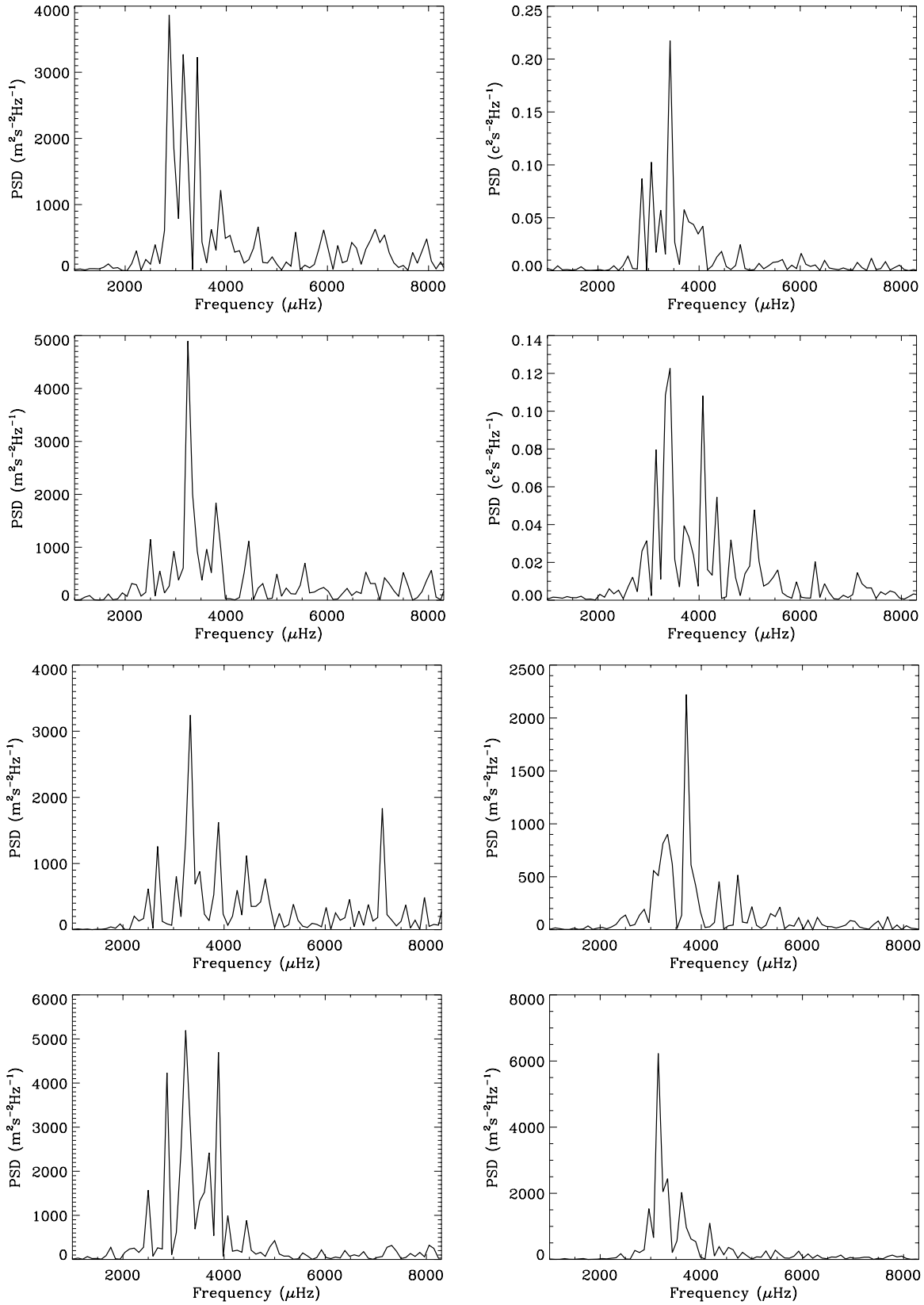

Figure 5. Fourier Power Spectrum (FPS) estimated from velocity time series. Left panels illustrate the FPS obtained from the three hours of the MDI data for the flare events of 2003 October 28 (during 10:00–13:00 UT), 2003 October 29 (during 19:00–22:00 UT), 2001 April 6 (during 18:00–21:00 UT), and a quiet period (non-flaring condition), respectively, from top to bottom. Right panels (from top to bottom) show the corresponding FPS obtained from the three hours of the GOLF data.

the Sun. Therefore, it is believed that the flare energy will have a larger relative effect at high frequency as the other sources of its excitation are much smaller. These observations open a new area of study concerning the excitation of global high-frequency waves by local tremors due to major solar flares. It would be interesting to correlate the epochs of enhancement of high-frequency waves with episodes of flare energy release, using a similar analysis with hard X-ray data. We defer this study to the future.

The use of data from the MDI and the GOLF instruments on board *SOHO* spacecraft is gratefully acknowledged. The *SOHO* is a joint mission under cooperative agreement between ESA and NASA. This work has been partially supported by the CNES/GOLF grant at the Service d'Astrophysique (CEA/Saclay). We are thankful to the referee for very useful suggestions which improved the presentation of this work. We are also thankful to Douglas Gough, John Leibacher, Frank Hill, P. Scherrer, Robertus Erdelyi, H. M. Antia, A. Kosovichev, and Christoffer Karoff for useful discussions related to this work.

REFERENCES

Ambastha, A., & Antia, H. M. 2006, Sol. Phys., 238, 219
Ambastha, A., Basu, S., & Antia, H. M. 2003, Sol. Phys., 218, 151
Balmforth, N. J., & Gough, D. O. 1990, Sol. Phys., 128, 161
Braun, D. C., & Duvall, T. L., Jr. 1990, Sol. Phys., 129, 83
Chaplin, W. J., et al. 2003, in SOHO 12 GONG+ 2002, Local and Global Helioseismology: the Present and Future, ed. H. Sawaya-Lacoste (ESA-SP 517; Noordwijk, Netherlands: ESA), 247
Chaplin, W. J., et al. 2004, Sol. Phys., 220, 307
Donea, A.-C., Braun, D. C., & Lindsey, C. 1999, ApJ, 513, L143
Donea, A.-C., & Lindsey, C. 2005, ApJ, 630, 1168
Fröhlich, C., et al. 1995, Sol. Phys., 162, 101
Gabriel, A. H., et al. 1995, Sol. Phys., 162, 61
Gabriel, A. H., et al. 1997, Sol. Phys., 175, 207
García, H. A. 1994, Sol. Phys., 154, 275
García, H. A., & Ballot, J. 2008, A&A, 477, 611
García, R. A., et al. 1998, ApJ, 504, L51
García, R. A., et al. 2005, A&A, 442, 385
García, R. A., et al. 2008, Sol. Phys., 251, 119
Gavryusev, V. G., & Gavryuseva, E. A. 1999, MNRAS, 303, L63
Goldreich, P., Murray, N., & Kumar, P. 1994, ApJ, 424, 466
Haber, D. A., Toomre, J., & Hill, F. 1988, in IAU Symp. 123, Advances in Helio- and Asteroseismology, ed. J. Christensen-Dalsgaard & S. Frandsen (Dordrecht: Kluwer), 59
Harvey, J., et al. 1995, in ASP Conf. Ser. 76, GONG'94: Helio- and Astero-Seismology from the Earth and Space, ed. R. K. Ulrich, E. J. Rhodes, Jr., & W. Dappen (San Francisco, CA: ASP), 432
Jiménez, A., et al. 2005, ApJ, 623, 1215
Jiménez-Reyes, S. J., et al. 2007, ApJ, 654, 1135
Karoff, C., & Kjeldsen, H. 2008, ApJ, 678, L73
Kosovichev, A. G., & Zharkova, V. V. 1998, Nature, 393, 317
Kumar, P., & Lu, E. 1991, ApJ, 375, L35
Kumar, B., & Ravindra, B. 2006, JA&A, 27, 425
Kumar, B., & Venkatakrishnan, P. 2009, in ASP Conf. Ser. 416, Solar-Stellar Dynamos as Revealed by Helio- and Asteroseismology, ed. M. Dikpati, T. Arentoft, I. González-Hernández, C. Lindsey, & F. Hill (San Francisco, CA: ASP), 331
Leibacher, J. W., & Stein, R. F. 1971, ApJ, 7, 191
Leighton, R. B., Noyes, R. W., & Simon, G. W. 1962, ApJ, 135, L474
Libbrecht, K. G. 1988, ApJ, 334, 510
Libbrecht, K. G., & Kaufman, J. M. 1988, ApJ, 324, 1172
Mathur, S., et al. 2008, A&A, 484, 517
Scherrer, P. H., et al. 1995, Sol. Phys., 324, 1172
Torrence, C., & Compo, G. P. 1998, BAAS, 79, 61
Ulrich, R. K. 1970, ApJ, 79, 61
Ulrich, R. K., García, R. A., & Robillot, J.-M. 2000, A&A, 364, 799
Venkatakrishnan, P., Kumar, B., & Uddin, W. 2008, MNRAS, 387, L69
Wolff, C. L. 1972, ApJ, 176, 833
Zharkova, V. V., & Zharkov, S. I. 2007, ApJ, 664, 573